Technology and Economics of Smart Grids and Sustainable Energy (2019) 4: 1
https://doi.org/10.1007/s40866-018-0059-4

ORIGINAL PAPER

Investigation of Energy Storage Batteries in Stability Enforcement of Low Inertia Active Distribution Network

K. N. Bangash[1] · M. E. A. Farrag[2,3] · A. H. Osman[1]

Received: 1 February 2018 / Accepted: 11 December 2018 / Published online: 2 January 2019

Abstract

The inherent intermittency of renewable power generation poses one of the great challenges to the future smart grid. With incentives and subsidies, the penetration level of small-scale renewable energy into power grids is sharply increasing worldwide. Battery energy storage systems (BESS) are used to curtail the extra power during low demand times. These energy storage systems are capable of absorbing and delivering real power to the grid. The increased penetration level of inverter-based distributed generation (DG) reduces the inertia of the grid and thus affects the transient stability of the network. This paper discusses and investigates the impact of BESS on distribution networks' stability with high penetration levels of inverter based DG. The obtained results show that proper charging and discharging schemes of the BESS can enhance the transient stability of the network. Fast switching between charging and discharging mode would be helpful during transient fault disturbance to keep the system in a balanced condition.

Keywords Renewable distributed generation · Energy storage battery · Low inertia distribution network · Transient stability

Introduction

Conventional power systems are dominated by large rotating turbines and synchronous generators, which provide the inertia and damping effects for stability requirements. A power system is known to be transiently stable if it is able to regain its stability after a disturbance [1]. The frequency of a large electric power system is maintained within an acceptable range by the rotational mass of many synchronous generators connected by tie-lines in the network [2]. The power system frequency is in a stable state when active power produced by generators is equally consumed by the total system load along with transmission and distribution network losses. This balance should be maintained as much as possible. During normal steady system operation, minor frequency deviations from its nominal value are common, but power system operator would always keep this deviation as low as possible. Synchronous generators and turbines provide the rotating mass and supply/consume kinetic energy to/from the electric grid during a frequency deviation, Δf. The supplied/consumed kinetic energy is proportional to the rate of change of the frequency [3]. During transient stability events, the inertia constant H of synchronous generator curtails the frequency deviation. This phenomenon slows down the frequency dynamics which increases the response time for transient events such as system faults, power plant outages, and sudden disconnection of loads. Penetration of inverter-based Renewable Energy Sources (RES) such as Photovoltaic (PV) units and wind turbines in power systems have been increasing rapidly over time. The increase of RES penetration results in an equivalent decrease in conventional generators and thus the rotational inertia in the system becomes very low. This can lead to serious effects on the system's frequency deviation [4].

The stored kinetic energy (E_{kin}) in the rotating mass of the conventional synchronous generator help regulates the frequency deviation by slowing down the frequency dynamics. The rotational energy is given as:

$$E_{\text{kin}} = \frac{1}{2} J (2\pi f_m)^2 \quad (1)$$

where J is the moment of inertia of synchronous generator and f_m is the frequency of the machine. The inertia constant H for a

✉ K. N. Bangash
kbangash@aus.edu

✉ M. E. A. Farrag
Mohamed.Farrag@gcu.ac.uk

[1] Electrical Department, American University of Sharjah, Sharjah, United Arab Emirates

[2] Department of Engineering, School of Engineering and Built Environment, Glasgow Caledonian University, Glasgow, UK

[3] Faculty of Industrial Education, Helwan University, Helwan, Egypt

synchronous machine is the ratio of the kinetic energy of rotating masses and generator rated power, given by:

$$H = \frac{E_{kin}}{S_B} = \frac{J(2\pi f_m)^2}{2S_B} \tag{2}$$

where H is the time typically in the range of 2~10 s, during which the machine can supply its rated power exclusively through its stored kinetic energy. The classical swing equation given in (3) describes the inertial response of the synchronous generator following a power imbalance.

$$\dot{E}_{kin} = J(2\pi)^2 f_{\mathrm{m}} \cdot \dot{f}_{\mathrm{m}} = \frac{2HS_B}{f_{\mathrm{m}}} \cdot \dot{f}_{\mathrm{m}} = (P_{\mathrm{mec}} - P_{\mathrm{e}}) \tag{3}$$

where P_{mec} is the mechanical power supplied by the generator and P_{e} as the electric power demand. The rotational inertia of the power system increases with the increase of the synchronous generators number. The inertia constant H is inversely proportional to the frequency dynamics. Therefore, the higher the inertia constant H the lower is the frequency deviation.

The high penetration level of inverter-based distributed generation (DG) with no rotating mass decreases the rotational inertia of power systems. Thus, low inertia inverter-based DG in small power networks would lead to high deviations in voltage and frequency during large disturbances [5]. The time frame for different frequency stability issues varies from a few seconds to several minutes or sometimes hours. Table 1 describes the time frame for potential frequency stability issues.

For system security, sufficient operational generation reserves are required to compensate for the unexpected loss of generation or sudden load rejection. The inadequate operational reserve would consequently lead to frequency instability that can trigger automatic load shedding. In European countries, whose networks are interconnected, standard EN 50160 specifies 50 Hz ±1% (49.5~50.5 Hz) for 95% of the week and [+4%, −6%] (52~47 Hz) in the event of major disturbances [7]. During low load consumption and renewable power generation is reasonably high, the load dispatcher may restrict or curtail energy generated from the renewable sources to maintain the system standard frequency within limits, which may be considered as a waste of energy [8]. Battery energy storage systems (BESS) can be used as a tool to absorb the unusable electric energy that generated by those sources and stream its power back to the grid during truncated generation. This will help the system to accommodate the average load scheme as a favor compared to peak load scheme. Peak demand on the UK grid is expected to severely increase by 2050 due to abrupt demand from electric vehicles market, especially after the adoption of no new petrol-based vehicles to be bought after 2030 and also due to household heating ascents. Energy storage technologies could produce savings of £10 bn a year by 2050 in the UK [9]. ABB and UK Power Networks developed a dynamic energy storage solution that supports power quality during disturbances and support intermittence of wind power generation [10].

Integration of renewable generation in the main grid can change the system reliability and security measures. System operator would always be busy to shut down or synchronize the conventional generator depending upon intermittency of the solar and wind power generation. This could alter the real and reactive power reserve that is required for system operation and stability. Wind farms are usually built at locations with strong winds. Thus, the selection of the wind farm location is limited and the grid has to be designed accordingly. High penetration of wind power production to existing grid system can overload transmission and distribution network [11–13]. Moreover, the operational switching combinations of embedded DG would make the fault current calculations more complex as compared when the power flow is one way and passive demand [14].

Power network is a composite system, which is susceptible to disturbances. The power system is transiently stable, if it remains intact in synchronism and survives after grid faults such as the short circuit in transmission lines. Transient stability depends on the type of disturbance like fault duration, fault type, operating conditions and system characteristics [15]. The rotor of synchronous generators must remain synchronized with the rotating magnetic field of the stator after a fault. The generators must come back into synchronism with the rest of the system after oscillations once the fault is cleared. If they cannot come back into synchronism, the generators will experience cascade tripping with an increased chance of blackout [16–18].

Nagaraju Pogaku et al. [19] developed the modeling of autonomous operation of inverter-based microgrids to analyze the

Table 1 Time Frame for frequency stability issues [6]

Time	Potential issues	Contribution
Few Seconds	Low system inertia, low primary control response time	Synchronous and asynchronous generators (and motors)
10–30 Seconds	Inadequate primary reserve Slow activation time of primary reserve	All primarily controlled generators in the system
5–15 min.	Inadequate secondary reserve Slow activation time of secondary reserve	Load shared by Generators in the area of disturbance is regulated by load dispatch center
More than 15 min.	Insufficient regulatory Reserve Activation is manual, no frequency response	All generators contracted for this service

oscillatory modes for its poor damping. The developed model includes inverter low and high-frequency dynamics, network dynamics and load dynamics. These inverter models allow achieving the required stability margin for reliable grid operation. Soni et al. [20] developed a controller for the inverters to regulate the frequency after large frequency deviations in microgrids. Anurag K Srivastava et al. [23] investigated the use of energy storage systems, such as batteries and ultra-capacitors to improve the transient stability of a system penetrated with DG. Small synchronous and induction generators are used to represent DG. Since these DG are not inverter-based DG, the inertia of the system has increased and thus the transient stability is improved. Sebastián and Alzola [24] presented the modeling and testing of an islanded Wind-Diesel Hybrid System (WDHS) with Ni–MH BESS. The constant speed stall controlled wind turbine generator comprises an induction generator is directly connected to the autonomous grid. The simulations show that the system dynamics are significantly improved by using BESS. Monshizadeh et al. [25] used a DC-side capacitor of the inverter as energy storage to mimic the kinetic energy of a synchronous generator. Though the DC-side capacitor is an essential element in most inverters, capacitors cannot supply power for a long time. Unlike capacitors, batteries can supply power for longer times. Jaber Alipoor et al. [26] used the alternating inertia technique to find the right value of the inertia using Virtual Synchronous Generator (VSG) to produce virtual acceleration or deceleration during oscillations. Soni et al. [20] proposed a control technique for inverter-based DG to improve the power management and frequency response of an isolated microgrid. The droop gain of the inverter is determined as a function of the frequency deviation. The inverter supplies higher power to add virtual inertia to the system and lower the frequency deviation.

One of the major concerns for using batteries is that they will degrade faster if also participate in grid operation, such as demand response, peak shaving and frequency regulation. Shi et al. [21] proposed a joint optimization framework for using BESS in both frequency regulation and peak shaving for commercial customers. The results show that cost savings are larger if batteries are used for multiple purposes rather than devoting them to a single application. Bian et al. [22] developed a method to estimate the demand side contributions to system inertia of Great Britain (GB) power system. Grid-connected synchronous motors in industries provide inertia. The demand side can contribute an average of 1.75 s inertia constant. However, the Variable Frequency Drives (VFD) used to control the motors decrease the demand side inertia though they help to enhance the efficiency. In the case of PV-systems and inverter based wind generators, the inverter acts like an active/reactive current source with no “rotor angle”, which could introduce transient rotor angle instability [27].

According to G83/2 and G59/1 Engineering Recommendations [28, 29], if the line-line voltage reaches 0.8 pu DG should remain connected to the grid for 0.5 s. The duration is increased to 2.5 s if the measured line-line voltage is 0.87 pu. The DG should not be tripped as long as the frequency is above 47 Hz and below 50.5 Hz as recommended by the Engineering Recommendation G83/2, G59/1 given in Table 2, [30, 31].

In this work, with the integration of inverter based DG, synchronous generator is disconnected for economic load dispatch. Transient stability is executed on Matlab and the ability of the remaining synchronous generator to recover back after a fault is analyzed. During high DG output power, Energy Storage battery (ESB) are required to be in a charged mode to allow for a higher share of real power production from SM, which leads to an increased kinetic energy and better stable operation. Energy storage battery is used to balance the generation and demand, and improve transient stability.

This research analyses the impact of extra penetration of inverter-based PVs and wind power at UK 11 kV distribution feeder, and its impacts on system stability. This paper is organized as follows; section I, describes the background information about the work and the impact of inertia-less DGs on system transient stability. Section II, illustrates the modeling of a UK distribution system with rooftop PVs and wind power generation. Section III, presents the transient analysis of DG and BESS. Finally, conclusions are presented in Section IV.

General Problem and System Description

A typical home load profile of UK on a bright sunny day during the summer season is used for simulation. The rooftop PV output power rating is 3 kW. The patterns of the daily load cycle, PV and wind power production are illustrated in Fig. 1 [32, 33]. The wind profile is obtained from a weather station that is attached to one of Caledonian Buildings in Glasgow.

In the UK, power demand is less than DG (PVs and Wind) power production, particularly at the middle of the day during the summer season. Moreover, during peak load timing, PV power production is null, while wind power generation drops down as shown in Fig. 1. High penetration of renewable DG can cause reverse power flow, which results in unpredictable short-circuit current. Therefore, changes in the settings of the installed protective relays are required. Moreover, single phase PV power production can cause unbalance voltage [34].

National grid centre would like to decommit expensive generator units for economic load dispatch during high

Table 2 Frequency protection settings [31]

Parameter	Trip setting	Trip time
Over frequency	50.5 Hz (50 Hz +1%)	0.5 s
Under frequency	47 Hz (50 Hz −6%)	0.5 s

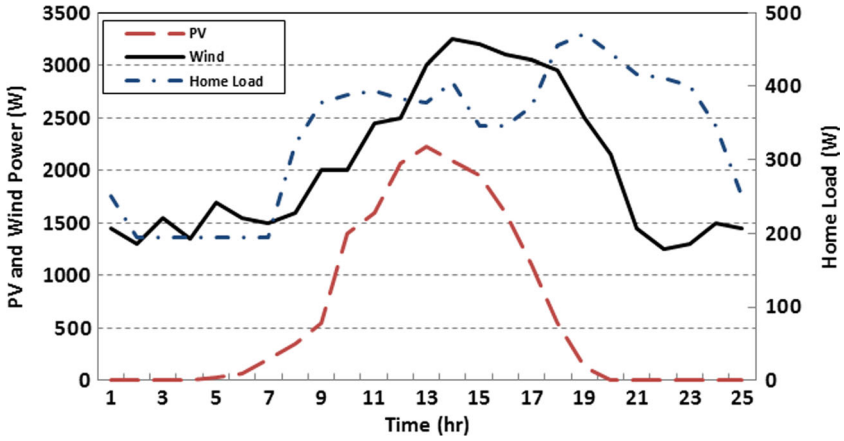

Fig. 1 Domestic load profile, PV and wind generation (average summer day)

renewable power generation and less load demand. The inertia of the system will be reduced by decommitting some synchronous machines from the power system. Sudden connection/disconnection of loads or temporary short circuits may lead to oscillations, and sometimes the remaining synchronous machines may lose synchronization from the system. The excessive electricity generated by the DG during low load consumption and high renewable power generation can be stored in the battery storage installed at the LV distribution network. This power can be supplied back during high power consumption times. In this paper, the use of BESS to enforce stability in low inertia systems is investigated. This can be the bi-product of batteries other than storage.

In the future smart grid, more and more renewable DG would replace conventional synchronous machines (SM). Power systems would also shift from centralized to decentralized topologies in the form of the microgrid. In a microgrid, the generation should be balanced with the load and the losses in the network. The generation in microgrids is composed of conventional SMs driven by diesel engines in addition to low-inertia renewable DG. In case of disturbance, the SMs in the microgrid may lose their synchronization due to the low inertia in the system. This challenge is investigated in this paper using a typical 11 kV UK distribution feeder with local conventional SMs. The feeder is disconnected from the main grid forming a microgrid. It is expected that renewable DG would be installed in the feeder and accordingly, the need for expensively operated SMs would be reduced. In this paper, the idea of home connected energy storage battery is used to cope with the stability issue due to the low inertia created by the high penetration of inverter-based renewable DG. During the charging mode of the batteries, the transient stability is increased, due to the increased share of power production from SM which increases the kinetic energy.

Synchronous generators of 2 MVA, 400 V, 50 Hz, 112 kg.m^2, 1500 rpm driven by a diesel engine are selected for simulation. Figure 2 describes the block diagram of the diesel engine generator set. The diesel engine is coupled with the synchronous machine. The engine's speed is maintained at 1500 rpm with speed regulator/governor. Increased real power load on the synchronous generator, results in an imbalance torque on the coupled synchronous generator rotor and the crankshaft. This results in deceleration of the engine and causes an equivalent reduction in generated frequency.

The engine speed regulator acts as a feedback controller and is used to regulate the engine's speed. The regulator responds by increasing the fuel rate, with this the engine's gross output torque is increased, resulting in the engine speed and frequency to run at rated value. The difference between the actual and desired speed is used as the input to the proportional, integral plus derivative (PID) controller as shown in Fig. 3. The regulator uses a discrete variable-gain PID controller to determine the desired quantity of fuel to be delivered to the next available cylinder.

The voltage regulator controls the field current to the exciter and keeps the generator voltage constant. Figure 4 depicts the voltage control system. The voltage regulator control system is implemented with a Proportional, Integral (PI) controller to stabilize the voltage by controlling reactive power (VAR). A sudden increase in generator real power results

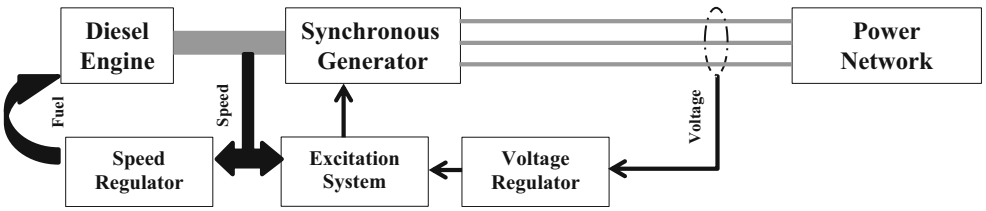

Fig. 2 Block diagram of diesel engine generator

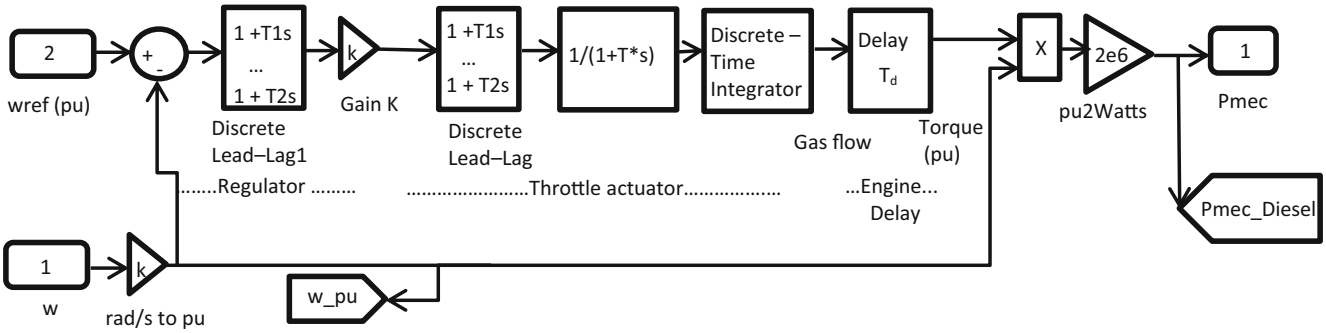

Fig. 3 Speed control system

loads torque higher than the engine torque. The engine speed decreases because the engine governor cannot respond quickly. Speed regulator increases the fuel supplied to the engine once deceleration is detected. The generated voltage is also proportional to engine speed so the generator terminal voltage decreases due to armature reaction and internal voltage drops. The voltage regulator compensates this drop by increasing the generator excitation field current.

Two synchronous generators are connected at one terminal of the UK feeder as shown in Fig. 5. The voltage regulator and the exciter control the voltage at the SMs' terminals. All these parameters are available in standard built-in models for SM in the power systems library of Simulink/Matlab. Lumped load representing domestic power consumption is connected at seven 11/0.4 kV, 500 kVA transformers. The consumer lumped load (cluster of 384 homes) consists of a 140 kW at each 11/0.4 kV distribution transformer. A 500 kW extra load is connected adjacent to the SMs bus. Single synchronous generator (2 MVA) is feeding a total of 1480 kW load while the home load is considered at unity power factor. The input from the inverter based DG is kept constant during a fault. Transient stability of the SM is investigated and hunting oscillation is observed.

DG power production is injected using a three-phase dynamic load block of Simscape power systems library [35]. The active reactive powers of the load are defined by an external Simulink® vector of two signals. By assigning a negative sign to external Simulink vector, three-phase dynamic load block can inject a prescribed amount of P and Q into the network. This can represent inverter based DGs in which the inverter controls the amount of P and Q generated by the variable speed/frequency wind turbines or the dc PV panels. The distribution network only receives P and Q from the inverter, and therefore, a detailed model of wind turbine and PV panels are not simulated in this work. BESS is considered as a source of active power consumption, three-phase dynamic load block is used to model ESB in Grid to Battery (G2B) mode. The negative sign is assigned to the output of the Simulink three-phase dynamic load block to model the BESS in Battery to Grid (B2G) mode. In the B2G mode, the battery is utilized to balance the frequency or avert stability margins by injecting active power into the system. The emulator with Li-ion battery characteristics was tested on IEEE-24 bus system using OPAL-RT real-time simulator [36]. The ESS showed 80 ms frequency response time for major imbalance while keeping the state of charge (SoC) to 50%. Almost, 100 ms time delay is used in this research, whenever the battery is switched from G2B into B2G mode. Small size Lithium-ion batteries ranging from 1 to 10 kWh are available to maximize the PV consumption by storing electricity during off-peak times [37]. ABB has worked with UK Power Networks to develop dynamic energy solution that ensures, power supply due to intermittent nature of renewable power, storing excessive renewable energy generation, improve power quality during fault and also afford dynamic voltage control for eight million homes and businesses in the UK [38].

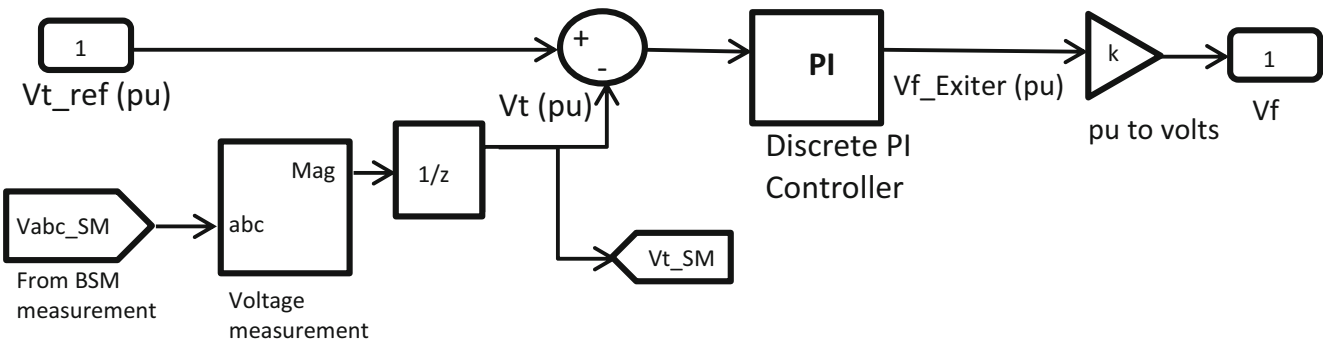

Fig. 4 Voltage regulator control system

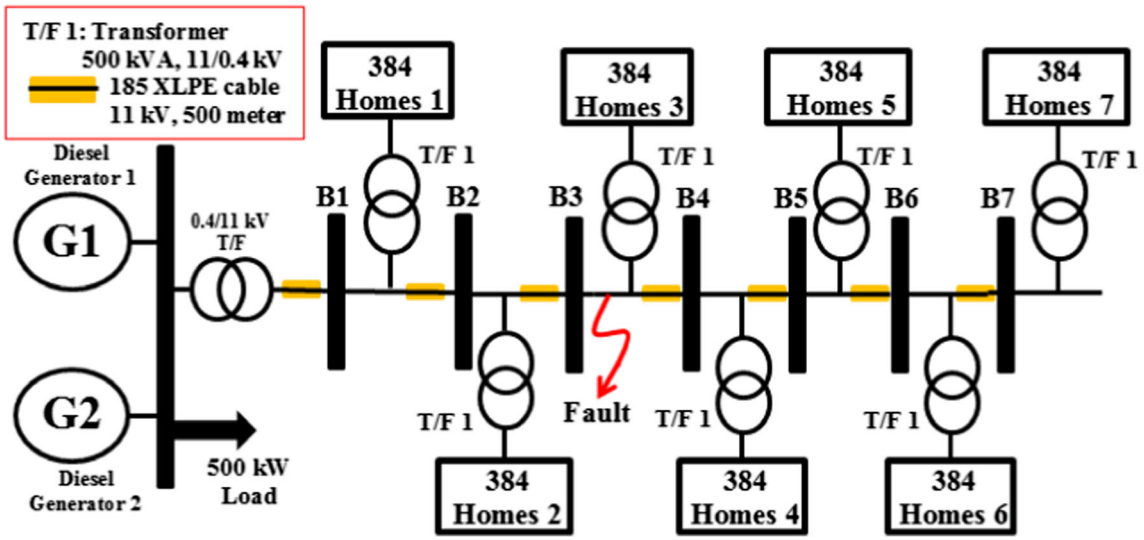

Fig. 5 Single 11 kV UK feeder with diesel generators and home load

Simulation Study

Base Case – Two SMs

A UK 11 kV feeder, shown in Fig. 5, is connected to two SMs driven by a diesel engine and simulated without DG. The performed simulations indicate that the critical clearing time for one SM without DG is 0.3 s while with two SMs connected, the critical clearing time is 2.0 s as the inertia of the system has increased. A three-phase temporary fault is applied between bus B3 and B4.

The fault is applied at $t = 5.0$ s and cleared at $t = 5.3$ s. The traces of P_{mec} representing the mechanical power of the SMs, the speed of the SM, frequency and fault location voltage are shown in Fig. 6a. During the short circuit, the mechanical power (P_{mec}) of the SMs drops down because the part of the feeder beyond the fault is no longer fed by SMs. P_{mec} does not recover back instantly, once the fault is removed due to the inertia. The power reached the maximum at $t = 5.7$ s and an oscillation is observed. During the fault, the frequency continued to increase and reached 51 Hz when the fault is cleared at 5.3 s. The two generators have enough synchronizing torques to remain in synchronism with the system when the fault is removed after 0.3 s. The voltage at the fault point is zero during the fault. Moreover, each SM contributed a fault current of 740 amps upon the occurrence of the fault and decreased to 600 amps when the fault is cleared.

Distribution Feeder with Two SM and DG

Two SMs are connected at one terminal of the 11 kV feeder and one DG of a capacity equal to the total domestic load (7 × 140 kW) is connected at the other end of the feeder, representing a wind farm as shown in the Fig. 7. The traces

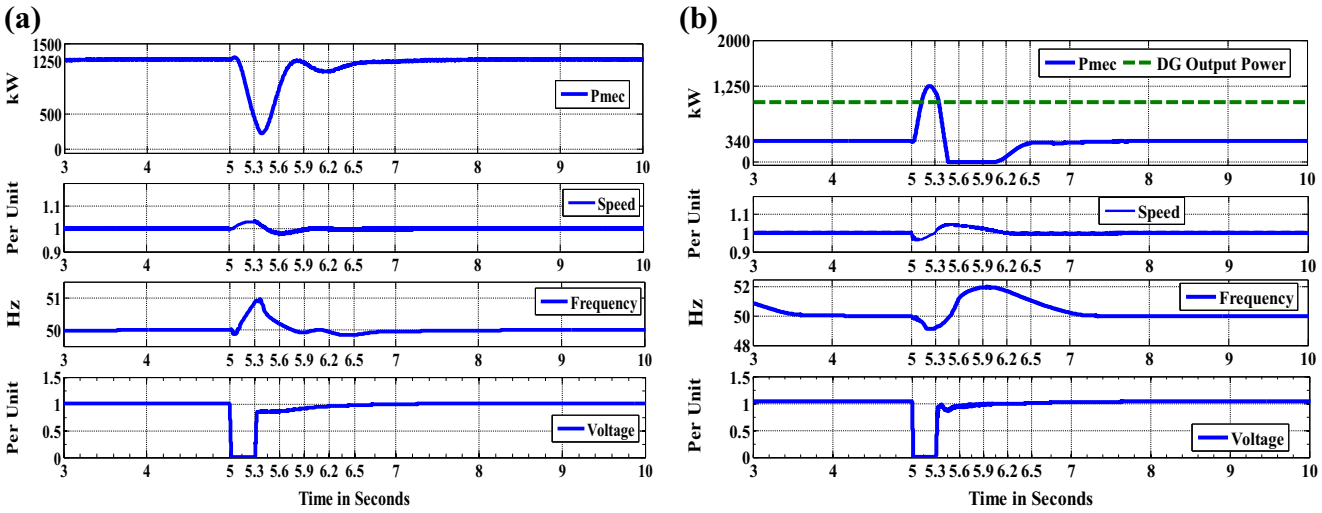

Fig. 6 Response of the generator power, speed, frequency and voltage before, during and after the fault

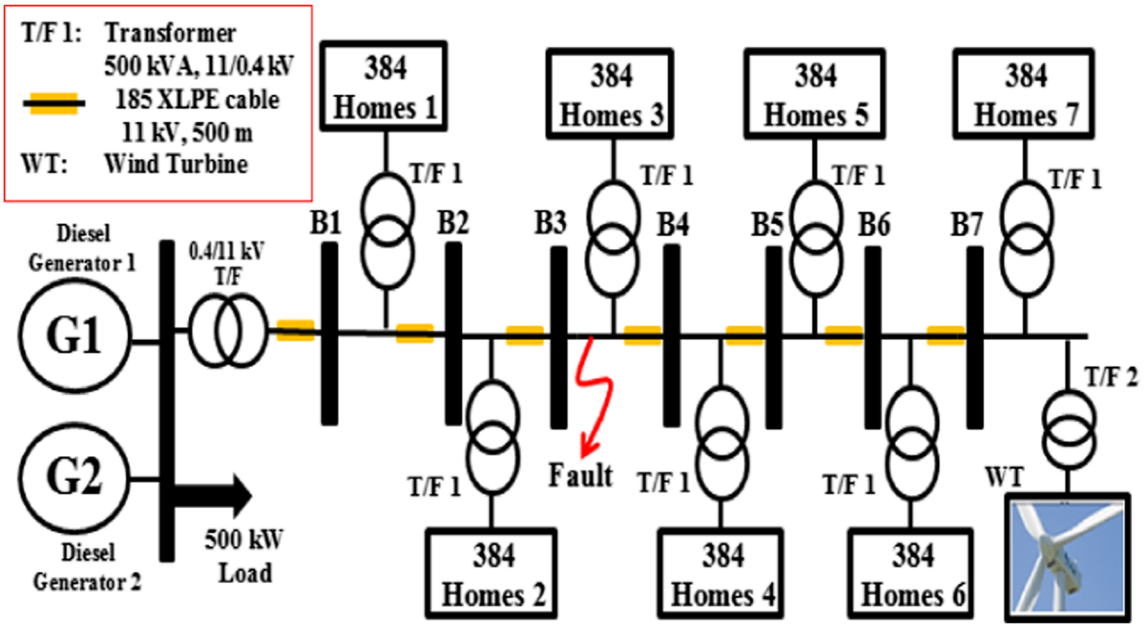

Fig. 7 Single 11 kV UK feeder with diesel generators and wind farm

of P_{mec} representing the mechanical power of the SM, DG output power, the speed of the SM, frequency and fault location voltage are shown in Fig. 6b. SMs and DG are delivering 340 kW and 980 kW respectively before the fault. During the short circuit, the SMs started to feed the bus up to the fault point that was previously fed by DG. P_{mec} increased from 340 to 1250 kW, while the speed and frequency dropped down. When the fault is cleared, the SMss power descended and due to inertia it did not settle at 340 kW but decreased to 0 kW. At $t = 6.1$ s, the SM power started to rise and stabilized at $t = 6.5$ s. The speed regulator maintains a speed of 1.0 p.u and nominal frequency to 50 Hz after a transient period of 1.5 s. The system is stabilized after 2 s.

The two generators have enough synchronizing torques to remain in synchronism with the system when the fault is removed at $t = 5.3$ s. Moreover, once the fault is cleared, the system experienced a power swing because the kinetic energy stored in the rotor increases the rotor speed. The frequency almost reached the maximum limit i.e. 52 Hz at $t = 5.6$ s. The traces of the DG output power also illustrates that the output power of inverter based DG is constant during the fault because the controller of the inverter does not allow power sharing as in SMs.

Fault Analysis with Low Inertia

One SM is replaced by wind turbine for economic load dispatch. A short circuit fault is applied at t = 5 s to investigate the system performance under the low inertia of the inverter based renewable DG. During the short circuit, a single generator with reduced inertia is hunting instead of supplying power to the feeder up to the fault point as shown in Fig. 8. Finally, P_{mec}

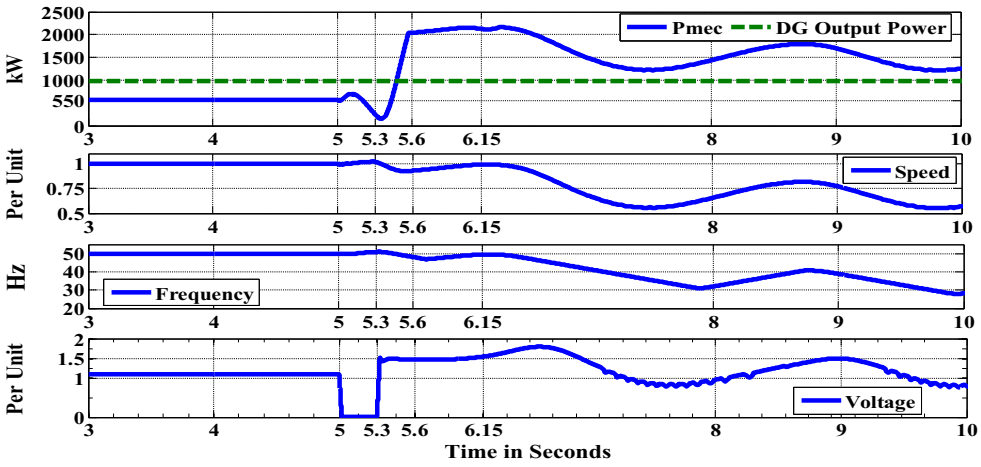

Fig. 8 Transient response of low inertia network without ESB

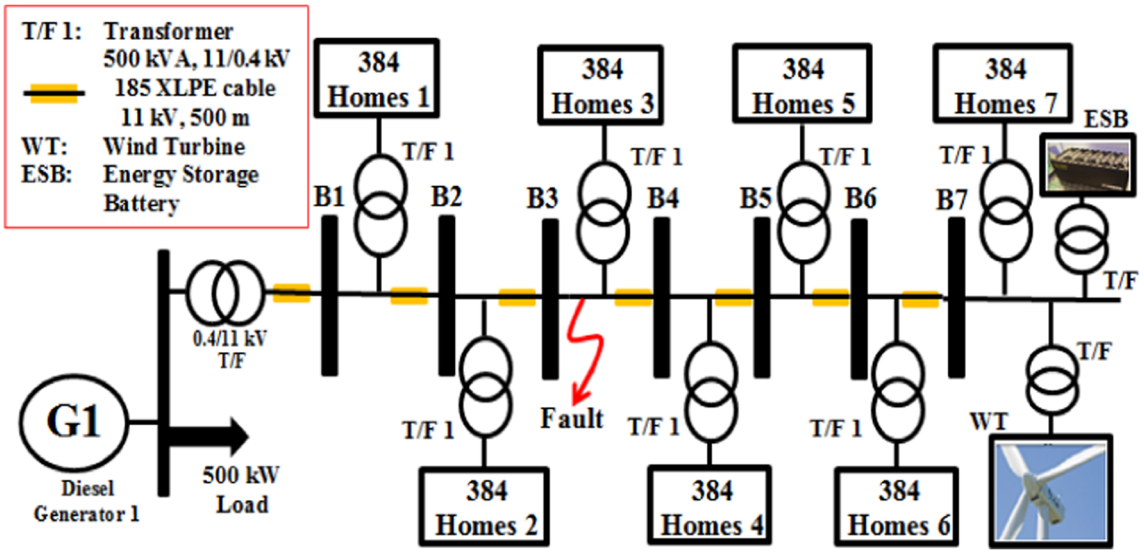

Fig. 9 Single 11 kV UK feeder with diesel generator, wind farm and energy storage battery

dropped down to 150 kW when the short circuit is cleared at $t = 5.3$ s. After the clearance of the short circuit, P_{mec} is supposed to return back to 550 kW, but with low inertia, it delivered maximum capable power. Speed and frequency oscillated till $t = 6.15$ s and then finally lost synchronism. With a low inertia system, the remaining SM was unable to regain synchronization back after the fault was cleared. The simulations performed on this configuration showed that the critical fault clearing time is 0.05 s. Moreover, the single SM contributed a fault current of 485 amps at the onset of the fault and decreased to 370 amps when the fault is cleared.

Impacts of Energy Storage Battery on Low Inertia Network

Energy storage battery (4x140kW) is connected besides the wind farm in charging mode as shown in Fig. 9. More than half of the power produced by the wind turbines is consumed by the batteries.

During the fault period, P_{mec} dropped down from 1120 kW since the SM is only feeding power to the fault point. Due to the low inertia, P_{mec} does not stop instantly and reached 0 at $t = 5.3$ s, as shown in Fig. 10. The frequency and the speed have increased because of the amount of electrical active power that the generator exports is not the same as the amount of mechanical power it imports. P_{mec} started to increase after the clearance of the fault and delivered its maximum power between $t = 5.7$ s to $t = 6.3$ s. At t = 6.3 s, P_{mec} started to decrease and settled to 1120 kW at $t = 10$ s.

It is obvious that when the fault is cleared, the impact of power flow from DG is less compared to the case where ESB are not used. Batteries are consuming the power produced by the DG. At t = 6 s the frequency reached 46.4 Hz with an initial dip of output power reaching zero. With the slow

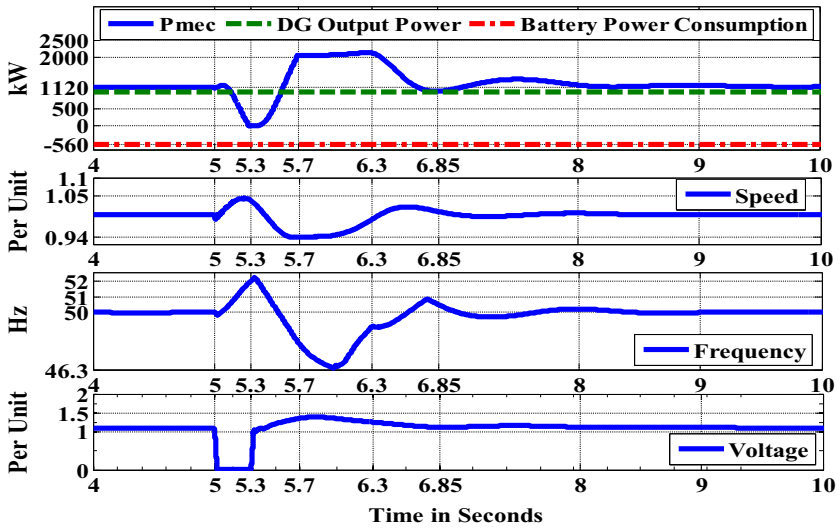

Fig. 10 Transient response of low inertia network with ESB

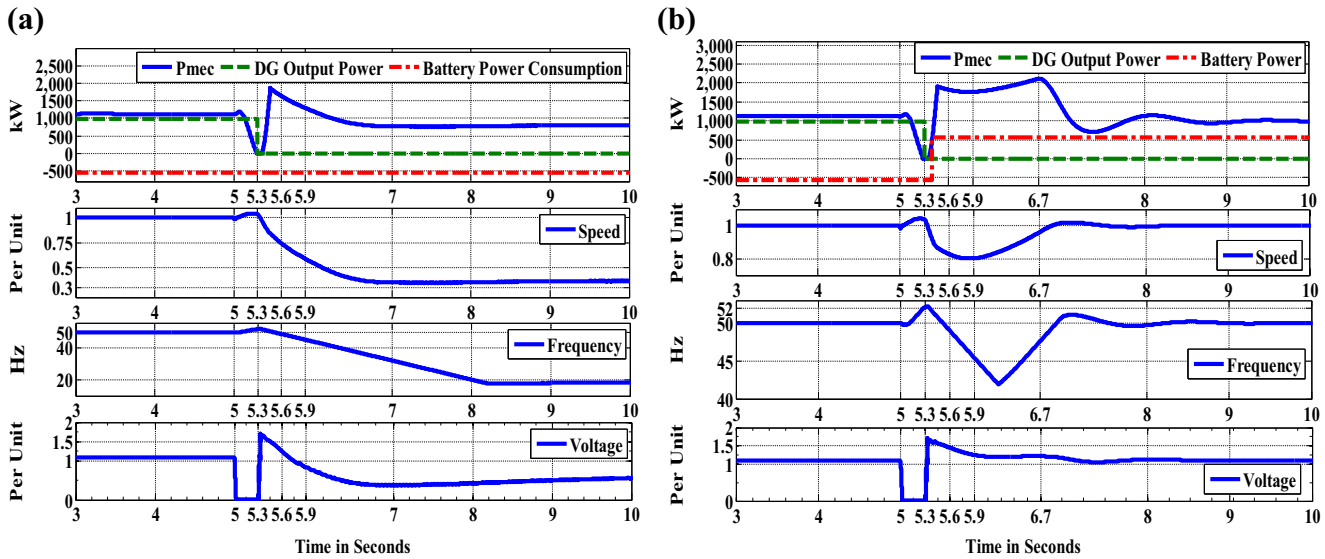

Fig. 11 Transient response with DG disconnected

hunting frequency, the SM is able to recover back. Once the fault is cleared, the machine speed begins to stabilize and the machine begins to export more active power (kW) compared to the pre-fault condition. This is because the machine has stored up kinetic energy in the rotor during the fault.

Transient Analysis with Disconnection of Wind Turbine

In this case, the wind DG is disconnected intentionally at the end of short circuit time i.e. $t = 5.3$ s, to investigate the stability of the system. Figure 11a shows the obtained results. When the DG is disconnected at $t = 5.3$ s, the SM takes the share of DG and P_{mec} increased to 1700 kW at $t = 5.5$ s. The rotor speed decreased and with low kinetic energy as well as active power reserve, it did not recover back and the SM is desynchronized. In the previous case, the system remained intact after the transient time because the battery load was incorporated. In the next case, the battery will be switched to the discharge mode i.e. battery to grid mode to analyze the impact of the battery on the stability.

Transient Response by Switching the Battery from G2B into B2G

In this case, the wind DG is disconnected intentionally at the end of the fault duration (t = 5.3 s) and the battery is switched from charging to discharging mode as shown in Fig. 11b. At $t = 5.4$ s, the battery delivered 500 kW to the system instead of consumption. Switching of the battery from −500 to 500 kW has injected 1000 kW to the system. The batteries have reduced the power demand from the system by 1000 kW that would increase the kinetic energy as per Eq. (3). The frequency dropped down to 43.5 Hz at $t = 6.3$ s but recovered back to 50 Hz at $t = 7.2$ s. With minor oscillation, the system is able to recover and become stable at $t = 10$ s.

Simulation is also performed to find the optimal power of ESB required in the G2B mode to keep the system synchronize after disturbance. ESB requires 40 kW of power in charging mode to keep the system stable and synchronized as depicted in Table 3. System stability and reliability is the bi-product of ESB, otherwise, the main function of ESB is to store excessive power and give back to the grid especially during peak hour load demand.

Table 3 Optimal ESB power to keep the system stable

ESB power (kW)	Synchronous machine status after the fault	Remarks
10	De-synchronized	ESB is connected adjacent to Wind farm/Solar park in the G2B mode
20	De-synchronized	
30	De-synchronized	
40	Synchronised	

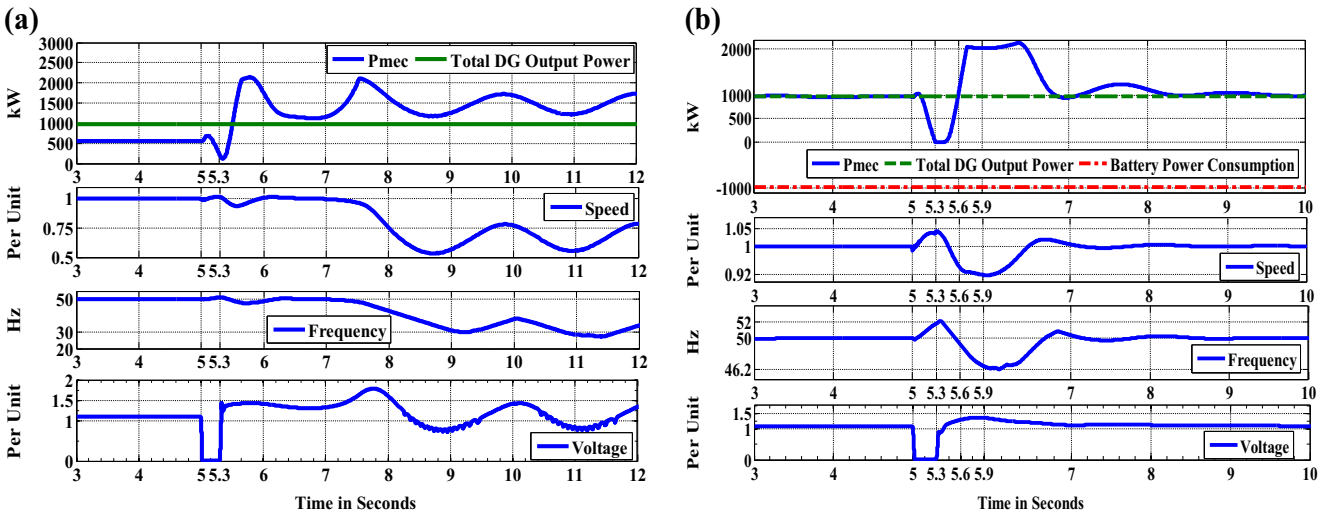

Fig. 12 Transient response with Roof top DGs

Roof-Top DG in Low Inertia System

In this case, a 140 kW capacity of DG is connected at the LV side of every 500kVA distribution transformer. This resembles domestic rooftop DG. The total power consumption is supplied by domestic renewable DG, which makes the power needed from the 500 kVA transformer negligible. Only one SM is connected in the system. With low inertia, the system is unable to stabilize after the fault clearance and desynchronized at $t = 7$ s as shown in Fig. 12a.

Impact of Roof-Top DG with Energy Storage Battery

A simulation is performed for the case when rooftop DG and batteries are connected to the system. At every LV side of the 500 kVA transformers, 140 kW batteries are connected in charging mode. Batteries consume 1000 kW extra power from the system. This has increased the electrical demand and consequently, P_{mec} of the synchronous generator has also increased to keep the generation and demand in balance. Thus, the kinetic energy has apparently increased. Less oscillation is observed after the fault clearance as shown in Fig. 12b. The system is recovered back to steady state condition at $t = 10$ s. The frequency is below 47 Hz for 0.5 s between $t = 5.84$ to $t = 6.34$ s. This result shows that with DG and batteries, the frequency fulfilled the frequency engineering recommendation given in Table 2. The batteries were able to recover back the system and eliminated the need to disconnect the DG which will lower the system frequency and deteriorates the conditions further.

Batteries in charging mode have increased the kinetic energy of SM as it has to increase its power to satisfy the demand. This property is useful for SM to resynchronize particularly in transient state conditions as illustrated in Table 4.

Simulation is performed for stability to find the total optimal power required by ESB in G2B mode. Rooftop DGs

Table 4 Comparison of scenarios

Scenario 1 Base Case 2 SM without DG	2 SM's have enough inertia to recover back after the fault is removed.
Scenario 2 Two SM and Inverter based DG	Oscillation is increased after the fault, as two ways of power flow, the share of power production from SM is low resulting in less kinetic energy, but the system has recovered back.
Scenario 3 One SM with Inverter based DG	The share of power production from SM is less and less kinetic energy. With low inertia, SM was unable to re-synchronize after the fault is removed.
Scenario 4 ESB is connected besides DG	The share of power flow from DG on the feeder is less as ESB is consuming the power produced by DG. SM is able to recover back because more power production that results in more kinetic energy.
Scenario 5 DG is disconnected	With Low active power reserve, SM does not recover back and ESB is still in charging mode.
Scenario 6 ESB switched from G2B into B2G mode	Switching ESB into B2G mode has injected real power into the system thus virtually injected inertia to the system. SM is able to resynchronize.
Scenario 7 Roof top DGs with one SM	Share of power production from SM is less so less kinetic energy. With low inertia, SM was unable to resynchronize after the fault is removed.
Scenario 8 ESB connected to Roof top DGs	ESB in charging mode has reduced the share of power from DGs and SM has gained kinetic energy by increasing power production. SM is recovered back.

Table 5 Optimal ESB power to keep the system stable with rooftop DGs

ESB power (kW) in individual LV feeder	Total ESB power (kW) of seven LV feeder	Synchronous machine status after the fault	Remarks
14	98	Synchronized	ESB is connected at every 11/0.4 kV transformer LV side in the G2B mode
7	49	Synchronized	
2.8	19.6	Synchronised	
1.6	11.2	Synchronised	
0.8	5.6	De-synchronized	

required 11.2 kW power of ESB to keep the system stable as shown in Table 5. This power is much less than the power required when wind farm with ESB is connected to one end of the feeder as described in Table 3.

Conclusion

In this research, the impact of the energy storage battery on the transient stability of the synchronous generator is analyzed. Firstly, the transient stability of UK 11 kV system with two SM is analyzed. With enough inertia and kinetic energy, SM is able to re-synchronize back and the system is stable. High penetration of inverter-based renewable DG would result in the shut-down of expensive, fossil fuel driven synchronous generators, resulting in low inertia and less kinetic energy. Transient stability of remaining generator is reduced and SM was unable to resynchronize after the fault is cleared. Oscillation and hunting were observed on rotor speed, frequency, voltage and mechanical power curve of the synchronous generator.

Secondly, ESB in charging mode during the high production of renewable DG has increased the load demand on the system this has increased the share of power from generator resulting more kinetic energy of the synchronous generators. Incorporation of ESB has effectively improved engine speed recovery during transient stability analysis. ESB is switched from charging to discharging mode in milliseconds to balance the generation and demand. Fast switching is helpful during transient fault disturbance to retain the stability of the system when any of the renewable DG is tripped.

Finally, the comparison is analyzed between rooftop scattered DGs and DG like wind farm/solar park connected at one end of the feeder. Rooftop scattered DGs with home connected ESBs, require less power to maintain stability as compared with wind farm connected ESB at one end of the feeder. Scattered DGs with ESB bring less variation on SM during transient stability state. ESB has improved transient stability thus the penetration level of renewable DGs can be further increased to reduce carbon footprints.

References

1. Kundur P, Paserba J, Ajjarapu V et al (2004) Definition and classification of power system stability. IEEE/CIGRE joint task force on stability terms and definitions. IEEE Trans Power Syst 19(3):1387–1401
2. Skopik F, Smith P (2015) Smart grid security innovation solutions for a modernized grid. Syngress I[st] edition
3. Kundur P (1994) Power system stability and control. McGraw-Hill Inc, New York
4. Ulbig A, Borsche TS, Andersson G (2014) Impact of low rotational inertia on power system stability and operation. Power Systems Laboratory, ETH Zurich. http://arxiv.org/pdf/1312.6435.pdf
5. Reza M, Slootweg JG, Schavemaker PH et al (2003) Investigating impacts of distributed generation on transmission system stability. IEEE power tech. In: Conference. Bologna, Italy
6. Heising K, Remler S (2013) Analysis of system stability in developing and emerging countries. Deutsche Gesellschaft für. In: Internationale Zusammenarbeit (GIZ) GmbH. Eschborn, Germany
7. Markiewicz H, Klajn A (2004) Voltage disturbances standard EN 50160 – voltage characteristics in public distribution systems. Copper development association
8. Sun T, Chen Z, Blaabjerg F (2003) Voltage recovery of grid-connected wind turbines after a short-circuit fault. In: 29[th] annual conference of the IEEE industrial electronics society. Virginia, USA
9. Ayasun S, Liang Y, Nwankpa CO (2006) A sensitivity approach for computation of the probability density function of critical clearing time and probability of stability in power system transient stability analysis. Elsevier, Applied Mathematics and Computation 176:563–576
10. Salman SK, Teo ALJ (2002) Investigation into the estimation of the critical clearing time of a grid connected wind power based embedded generator. Proceedings of the Asia Pacific IEEE/PES transmission and distribution Conference and Exhibition 11:975–980
11. Muyeen SM, Al-Durra A, Hasanien HM (2013) Modelling and control aspects of wind power systems. Ahmed G. Abo-Khalil Impacts of wind farms on power system stability. Ch-7, INTECH
12. Naimi D, Bouktir T (2008) Impact of wind power on the angular stability of a power system. Leonardo Electronic Journal of Practices and Technologies: issue 12:83–94
13. Morales JM, Conejo AJ, Ruiz JP (2009) Economic valuation of reserves in power systems with high penetration of wind power. IEEE Trans Power Syst 24(2):900–910

14. Ustun TS, Ozansoy C, Zayegh A (2013) Fault current coefficient and time delay assignment for microgrid protection system with central protection unit. IEEE Trans Power Syst 28(2):598–606
15. Amroune M, Bouktir T (2014) Effects of different parameters on power system transient stability studies. Journal of Advanced Sciences & Applied Engineering:28–33
16. Lew D, Bird L, Milligan M, et al (2013) Wind and solar curtailment. NREL, International workshop on large-scale integration of wind power into power systems as well as on transmission networks for offshore wind power plants, London, England
17. Selwa F, Djamel L (2017) Transient stability analysis of synchronous generator in electrical network. International Journal of Scientific & Engineering Research 5(8):55–59
18. Patel M, Soni N (2016) Assessment of transient stability of power system by using equal area criteria. International journal of modern engineering and research. Technology 3(4):38–44
19. Pogaku N, Prodanovic M, Green TC (2007) Modelling, analysis and testing of autonomous operation of an inverter-based microgrid. IEEE Trans Power Electron 22(2):613–625
20. Soni N, Doolla S, Chandorkar MC (2013a) Improvement of transient response in microgrids using virtual inertia. IEEE transactions on power delivery 28(3):1830–1838
21. Shi Y, Xu B, Wang D, Zhang B (2017) Using battery storage for peak shaving and frequency regulation: joint optimization for Superlinear gains. IEEE transactions on power systems: DOI 33: 2882–2894. https://doi.org/10.1109/TPWRS.2017.2749512
22. Bian Y, Wyman-Pain H, Li F, Bhakar R, Mishra S, Padhy NP (2017) Demand side contributions for system inertia in the GB power system. IEEE transactions on power systems: DOI 33: 3521–3530. https://doi.org/10.1109/TPWRS.2017.2773531
23. Srivastava AK, Kumar AA, Schulz NN (2012) Impact of distributed generations with energy storage devices on the electric grid. IEEE Syst J 6(1):110–117
24. Sebastián R, Alzola RP (2011) Simulation of an isolated wind diesel system with battery energy storage. Electr Power Syst Res 81(2): 677–686
25. Monshizadeh P, Persis CD, Stegink T, Monshizadeh M, Schaft AVD (2017) Stability and Frequency Regulation of Inverters with Capacitive Inertia. Computer Science, Systems and Control, Cornel University Library. https://arxiv.org/pdf/1704.01545.pdf
26. Alipoor J, Miura Y, Ise T (2015) Power system stabilization using virtual synchronous generator with alternating moment of inertia. IEEE journal of Emerging and selected topics in power electronics 03(2):451–458
27. Eftekharnejad S, Vittal V, Heyd GT et al (2013) Impact of increased penetration of photovoltaic generation on power system. IEEE Trans Power Syst 28(2):893–901
28. Gatta FM, Iliceto F, Lauria S, et al (2003) Modelling and computer simulation of dispersed generation in distribution networks. Measures to prevent disconnection during system disturbances. Proc. of IEEE Power Tech. Conference, vol. 3, Bolonga, Italy
29. Engineering Recommendation (2012) Recommendations for the connection of type tested small-scale embedded generators (up to 16A per phase) in parallel with low-voltage distribution systems. Operations Directorate of Energy Networks Association, London. Engineering Recommendation G83(2)
30. Jennett KI, Booth CD, Coffele F et al (2015) Investigation of the sympathetic tripping problem in power systems with large penetrations of distributed generation. IET Generation, Transmission & Distribution 9(4):379–385
31. Emhemed AS, Crolla P, Burt G (2011) The impact of a high penetration of LV connected micro generation on the wider system performance during severe low frequency events. 21st International Conference on Electricity Distribution, CIRED, Frankfurt
32. Barbier C, Maloyd A, Putrus G (2007) Embedded controller for LV network with distributed generation. Department of Trade and Industry (DTI) project, Contract number: K/EL/00334/00/REP, UK
33. Ali S, Pearsall N, Putrus G (2013) Using electric vehicles to mitigate imbalance requirements associated with high penetration level of grid-connected photovoltaic systems. 22nd International Conference on Electricity Distribution, Stockholm
34. Manditereza PT, Bansal R (2016) Renewable distributed generation: the hidden challenges – a review from the protection perspective. Elsevier, Renewable and Sustainable Energy Reviews 58: 1457–1465
35. The MathWorks, Inc. SimPower Systems, Simulink (built upon Matlab) Block Library http://www.mathworks.com/access/helpdesk/help/toolbox/physmod/powersys/
36. Greenwood DM, Limb KY, Patsios C et al (2017) Frequency response services designed for energy storage. Elsevier Applied Energy 203:115–127
37. From Kilowatt to megawatt Samsung has a solution", Energy Storage System (ESS), Samsung SDI, 2014. [Online]. Available: http://www.samsungsdi.com/ess/overview
38. Overview brochure "Energy Storage Keeping smart grids in balance" Power and productivity for better world, ABB